

Design, Analysis, and Testing of a Carbon Fibre-based Solid Rocket Motors

C. Rakeshkumar^{1,*}, Siya Singh², A. Surenderpaul³, C. Anand⁴, C. Kowsalya⁵

Abstract

The goal of the research is to simulate the outer shell of a rocket in order to fulfil mission criteria. Case failures can occur for a number of causes, including poor material selection, carelessness in the service conditions, inadequate non-destructive testing during crucial stages of production, and poor design and analysis. For this reason, it is crucial to simulate rockets with precise design and analysis. The study entails the designing of rocket case using Catia V5, modelling the rocket in Ansys Fluent 19.2 for aerodynamic analysis to simulate the flow around the rocket. Static structural analysis is carried out with Abaqus 6.14, where three different materials Carbon epoxy fibre, Kevlar epoxy fibre and Carbon-Kevlar fibre are selected. The result analysis focuses on the deformation observed under identical loading conditions across three distinct materials. Following this examination, the most appropriate material for fabricating the rocket structure is determined based on the findings. It is revealed that the Carbon-Kevlar composite exhibits the most favourable characteristics, making it the top choice for constructing the rocket. As a result, the Carbon-Kevlar composite is chosen and then fabricated for incorporation into the rocket's structure. To ensure the reliability of the rocket under real-world conditions, rigorous testing was conducted near the seashore. These tests included parachute deployment and ignition trials, designed to simulate flight conditions and evaluate both the structural integrity and overall functionality of the system. The results confirm that the Carbon-Kevlar composite is well-suited for aerospace applications, ensuring optimal performance under high-stress environments.

Keywords: Carbon-epoxy, kevlar-epoxy, rocket structural analysis, aerodynamic analysis, Solid rocket motor.

INTRODUCTION

A rocket is a vehicle that uses controlled explosions of propellant to generate thrust and propel itself

*Author for Correspondence

C. Rakeshkumar
Email: rakeshae0843@gmail.com,

^{1,2}Assistant Professor, Department of Aeronautical Engineering, Vel Tech Rangarajan Dr. Sagunthala R&D Institute of Science and Technology, Chennai, Tamil Nadu, India.

³Assistant Professor, Department of Aeronautical Engineering, Tagore Engineering College, Chennai, Tamil Nadu, India.

⁴Assistant Professor, Department of Aeronautical Engineering, Agni College of Technology, Chennai, Tamil Nadu, India.

⁵Research Scholar, Department of Mathematics, School of Advanced Sciences, VIT University, Chennai, Tamil Nadu, India.

Received Date: October 03, 2024

Accepted Date: January 28, 2025

Published Date: February 15, 2025

Citation: C. Rakeshkumar, Siya Singh, A. Surenderpaul, C. Anand, C. Kowsalya. Design, Analysis, and Testing of a Carbon Fibre-based Solid Rocket Motors. Journal of Polymer and Composites. 2025; 13(Special Issue 2): S650–S669p.

through the atmosphere or outer space. The basic principle behind a rocket's operation is Newton's third law of motion, which states that for every action, there is an equal and opposite reaction. As the rocket's engines expel mass at high velocity in one direction, an equal and opposite force, known as thrust, propels the rocket in the opposite direction. The history of rockets begins in ancient China, where rockets were used primarily for warfare and pyrotechnics. Early gunpowder-fuelled "fire arrows" set the foundation for the development of more powerful rockets over centuries. Scientists like Konstantin Tsiolkovsky in Russia and Robert Goddard in the United States laid the theoretical groundwork for modern rocketry, paving the way for the revolutionary V-2 rockets developed by Germany during World War II. These advancements formed the cornerstone of the Space

Age, culminating in the launch of Sputnik 1 in 1957 and the Apollo 11 moon landing in 1969. Today, rockets continue to be instrumental in space exploration, satellite launches, and even intercontinental ballistic missile (ICBM) technology. Full-scale rockets operate in the complex realm of high-altitude aerodynamics and extreme structural loads, model rockets provide a valuable platform for understanding the fundamental principles of rocketry at a smaller scale.

The structure of air flow through a rocket and its impact on drag and stability are described by rocket aerodynamics. In the domain of rocket aerodynamics, streamlined configurations are crucial for reducing drag, enhancing efficiency and guaranteeing effective ascent. Control surfaces and thrust vectoring mechanisms offer precise control over rocket's trajectory and orientation during flight. During re-entry into Earth's atmosphere, a rocket experiences extreme heat due to the intense friction between the air molecules and the vehicle's surface. This heat can reach temperatures of several thousand degrees Celsius, enough to melt or damage conventional materials. Some rockets employ active cooling systems, such as circulating coolant or flowing cryogenic fluids, to dissipate heat and maintain safe temperatures within critical components. Specialized materials such as ablative shields or thermal tiles are used to absorb and dissipate heat away from the vehicle's structure. The rocket's structural design must be robust enough to withstand the stresses experienced throughout its flight, without compromising its integrity. This involves using materials capable of withstanding high temperatures and designing structural components to distribute heat evenly. Additionally, the structural design must account for other forces such as aerodynamic loads, vibrations, and acceleration, ensuring that the rocket remains structurally sound and stable throughout its journey.

Rocket System

A rocket's structural system consists of the nose cone, control fins, and cylindrical body, which together form the rocket's frame. The exterior ballistics of a rocket are greatly influenced by the airflow parameters, which include velocity, flow rate, pressure, and drag force. Dimensionless quantities called aerodynamic coefficients, like lift and drag coefficients are used to evaluate a structure's aerodynamic behaviour. Instead of being generated from the forces alone, they are derived from the ratio of several forces. The primary causes of these aerodynamic forces are changes in viscous shearing stresses and pressure. An item traveling through a fluid medium experiences drag, which is described by a structure's drag coefficient. As a result, this particular parameter directly impacts the thrust characteristics of a rocket engine. Similarly, the relationship between the lift force and the product of dynamic pressure and area is represented by the lift coefficient. The direction of the airflow is perpendicular to the lift force's action. A pressure differential between the structure's top and lower surfaces is necessary for lift to be produced. The structural system's roles include transferring loads from forces produced during flight and supplying minimal aerodynamic drag for atmospheric flight. Structures for rockets need to be lightweight yet robust. The weight of the structure has a direct impact on the rocket's performance. A rocket's structural weight can be described using a range of mass ratios. The rocket's center of gravity is influenced by the structural weight distribution, which also has an impact on the rocket's stability and control.

Basic Structural Design Requirements

Structures for rockets are desired to be lightweight and have strong mechanical properties. The reason for the demand of light weight is that rocket needs to overcome its own weight against the gravity which in turn creates drag so the weight of the structure is directly related rocket's performance. The casing of the rocket should be such that it must support the structural loads exerted on it. It must be able to support the weight of the payload, propellant, and engine. For reducing the drag on the rocket, the body of the rocket is made suitable for the supersonic and hypersonic flight speeds.

LITERATURE SURVEY

Srinivas et al. [1] conducted an in-depth aerodynamic and flow analysis of single, double, and multistage rockets using ANSYS software to evaluate critical efficiency performance parameters such as pressure, temperature, density, and velocity at different Mach speeds. Their study identified optimal

Mach numbers for different configurations, with single-stage rockets performing best at Mach 4 and double-stage rockets at Mach 6, highlighting the significance of matching Mach speeds with stage configurations to minimize aerodynamic losses and improve propellant efficiency. Specifically, the analysis indicated a reduction in aerodynamic drag by up to 15% under optimal conditions, providing a significant enhancement in the performance and design of rocket propulsion systems. Aytaç et al. [2] explored the aerodynamic behaviour of subsonic rockets utilizing Computational Fluid Dynamics (CFD) to analyse the influence of various parameters on drag coefficient. Their findings underscore a significant sensitivity of drag force to changes in Mach number, revealing that a 30% increase in Mach number can result in a drag coefficient rise of nearly 70%. The study also compared the efficacy of different turbulence models, showing a 12% variation in drag coefficients between $k-\omega$ and $k-\omega$ SST models, thereby highlighting the critical role of choosing the appropriate turbulence model in rocket design to ensure accurate aerodynamic predictions. Fedaravičius et al. [3] investigated the aerodynamic characteristics of a rocket-target for the "Stinger" system, focusing on nose shape optimization. Using CFD techniques in ANSYS CFX software, airflow simulations around rockets with various nose shapes were conducted. The study analysed pressure contours, airflow streamlines, and drag characteristics at different velocities. Results indicated that rockets with conical noses exhibited the highest drag force across all velocity ranges, while elliptical noses demonstrated the lowest drag force at Mach 0.8. Consequently, the elliptical nose shape was deemed optimal for further rocket-target development. Sahbon et al. [4] conducted a CFD study on the Grot rocket to investigate the effect of motor operation on its aerodynamic parameters. Two series of simulations were performed: one with the motor inactive and the other with active thrust. The study focused on quantifying the changes in drag coefficient during thrusting phases and analysing the influence of Mach number on drag. Results indicated non-linear dependencies and emphasized the importance of considering pressure forces on the nozzle exit and aft end regions in drag coefficient variations. Additionally, comparisons with semi-empirical models showed good agreement in the supersonic domain.

Tun et al. [5] utilized CFD in SolidWorks to predict the aerodynamic coefficients of a 122 mm rocket, aiming for enhanced accuracy in flight simulation. Their study encompassed comparing results with those obtained through empirical methods. While the analyses showcased near parity between CFD and empirical outcomes, discrepancies were noted in the subsonic and supersonic regions for axial force coefficients and static stability coefficients. Despite the time-intensive nature of CFD computations, the method provided more precise results, with differences of about 31% in the subsonic range and good agreement in the transonic region. The investigation revealed insights into airflow patterns and pressure distributions, contributing valuable data for aerodynamic coefficient predictions essential for rocket flight dynamics. Peng et al. [6] conducted numerical simulations on the aerodynamic characteristics of a guided rocket projectile using FLUENT CFD software. The study investigated variations of lift and drag coefficients with Mach numbers and angles of attack, revealing that both coefficients rise with increasing angles of attack and change rapidly in the transonic zone but smoothly in subsonic and supersonic regions. Notably, the analysis highlighted the significant influence of canard deflection on the flow field near tailfins, with vortices developed at the root of canards impacting flow interaction between canards and tailfins. Manimaran et al. [7] investigated the stability analysis of a conventional rocket model using CFD tools to determine the centre of pressure (CP) and centre of gravity (CG), crucial for predicting stability. Results revealed a stable rocket with a 2.75 calibre stability, denoting efficient aerodynamic stability. The study emphasized the significance of maintaining a sufficient distance between CP and CG to ensure stability throughout the rocket's trajectory, particularly as the CG shifts due to propellant combustion.

Dahalan et al. [8] conducted an aerodynamic study of a curved fin rocket using a combination of semi-empirical methods and numerical simulation, aiming to predict aerodynamic characteristics. Results from wind tunnel testing, USAF DATCOM analysis, and CFD simulations exhibited similar trends in normal force and drag coefficients, with CFD results closely aligning with wind tunnel data. The study highlighted the efficacy of CFD as a cost-effective alternative to wind tunnel testing, providing accurate predictions of lift and drag coefficients for curved fin rockets. The CFD simulations

demonstrated a reduction in drag coefficients by approximately 15% compared to USAF DATCOM analysis.

Robinson et al. [9] presented a comprehensive structural analysis of a two-stage fully reusable Advanced Manned Launch System (AMLS) vehicle, focusing on near-term material technology. The study emphasizes the importance of early structural analyses to assess the impact of evolutionary material technologies and mitigate program risk. Structural efficiency is highlighted through the resizing of elements to enhance global buckling strength, reducing weight by optimizing load paths. The paper underscores the sensitivity of fully reusable launch vehicle concepts to weight growth, urging for detailed structural analyses to optimize design and minimize structural weight, thus enhancing overall efficiency and feasibility.

Thankachen et al. [10] discuss stress analysis in rocket structural design, leveraging numerical software for simulation-based safety estimation. Their study optimizes a test rocket structure for aerodynamic loads, detecting stress concentration in fin and blade regions. Design optimization adjusts thickness in these areas, yielding improved structural integrity. Results indicate significant stress reduction, ensuring all stresses remain within specified limits or below material yield stress. Furthermore, factor of safety calculations demonstrate adherence to design specifications, with values exceeding the required threshold of 1.4. Capra et al. [11] conducted a comprehensive aerothermal-structural analysis on a Mach 8 scramjet experiment, assessing internal flow path and atmospheric conditions. The study revealed elevated surface temperatures during descent, particularly affecting the leading edge and inlet-combustor assembly. Despite these challenges, transient stresses remained low, with only minor regions exceeding material limits. Notably, common engineering materials like copper and carbon phenolic demonstrated resilience, showcasing their suitability for high-speed scramjet engines. This analysis underscores the importance of meticulous design and detailed analysis in ensuring structural integrity under extreme hypersonic heating conditions. Shaik et al. [12] explore the use of carbon-epoxy IM10/8552 composite in rocket motor casings, comparing it with traditional D6AC steel. Their research, conducted through various simulations in ANSYS 15.0, including static structural, steady-state thermal, and linear buckling analyses, indicates significant advantages of the composite material. The carbon-epoxy composite demonstrated higher stress and deformation tolerance, lower heat flux, and superior buckling resistance compared to steel, highlighting its efficiency and suitability for aerospace applications. The most effective layup for this composite was identified as [0/90/45/-45/90/0], showcasing its potential for enhancing rocket motor casing design. J. Jensi Joshua et al. [13] conducted an in-depth study on the mechanical properties of Kevlar-Glass/Epoxy interwoven composite laminates, exploring different weaving patterns (1x1, 3x3, and 5x5) to determine their impact on strength and durability. Their findings indicated that the 1x1 weaving pattern exhibited the highest tensile, compressive, and flexural strengths, making it particularly suitable for aerospace and transportation applications. The 5x5 pattern showed superior shear strength and fracture toughness, while the 3x3 pattern excelled in impact strength, suggesting its potential use in bulletproof vests and aerospace components [14]. In the study by Kothamasu Kiran et al., the specific numerical details regarding the percentage change in structural parameters due to variations in Mach numbers are not detailed in the abstract provided. However, the general findings indicate that as Mach numbers increased from 1.5 to 3, there was a significant increase in structural deformations and a corresponding decrease in normal forces. These changes highlight a substantial impact on the rocket's structural integrity and aerodynamic stability under higher speeds [15]. Habaka et al., the focus was on investigating the vibration characteristics of a full-scale free-flight missile with a 70mm calibre. The study aimed to understand the dynamic behaviour of the missile to enhance flight performance without compromising structural rigidity. Through experimental modal analysis using accelerometer sensors and numerical analysis with ANSYS Workbench, the study successfully identified the first four bending modes and their corresponding natural frequencies, showcasing a close agreement between experimental and numerical results.

METHODOLOGY

Design Consideration

In order to optimize efficiency and save expenses, the outer shell arrangement is deemed to be the best or optimal envelope. The payload, inter-stage connecting structures, handling equipment, launch facilities, usage of a certain propellant combination, and auxiliary equipment can all be taken into consideration while determining the final shell configuration.

Rocket 3D Modelling

Single staged model rocket for the analysis has been considered. The CAD model of the rocket has been designed in CATIA V5. The dimensions for the design are shown in the Figure 1-A, 1- B, 1- C, and 1-D below:

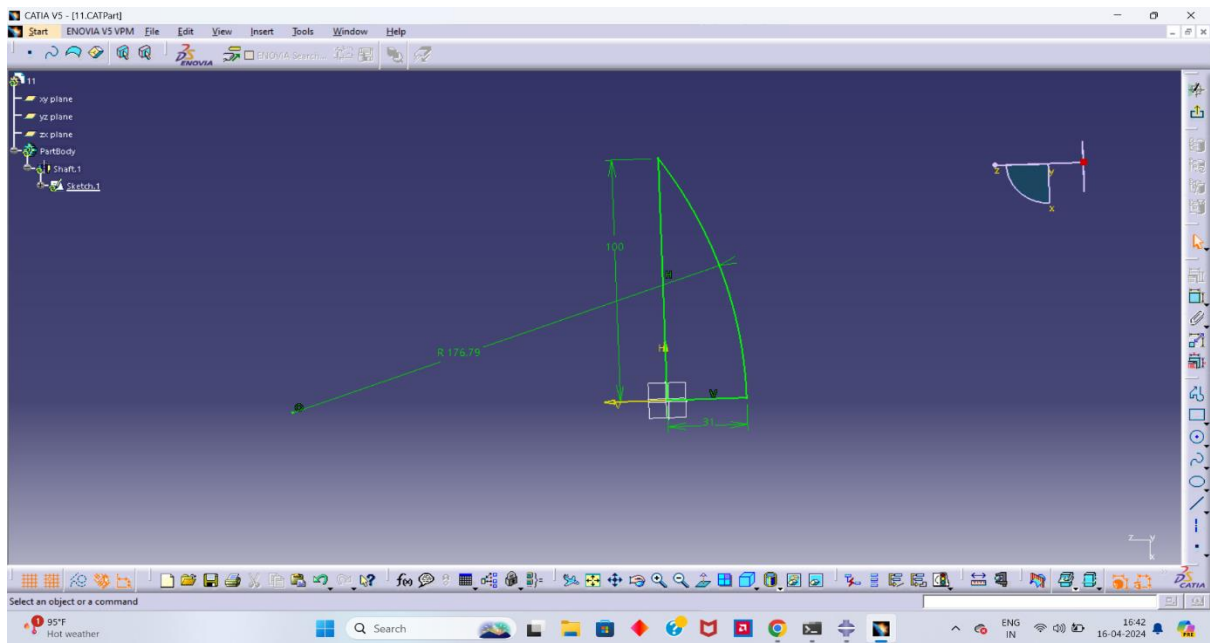


Figure 1. (a) O-give nose cone cross-section.

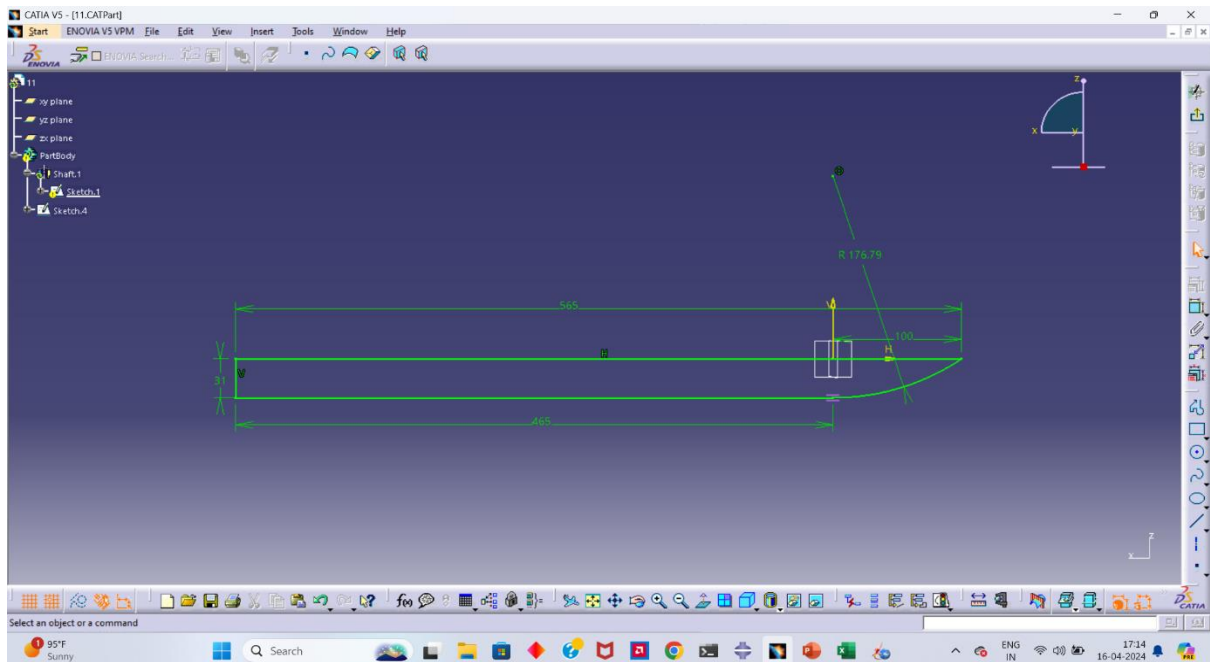


Figure 1. (b) Cross-section of body of rocket

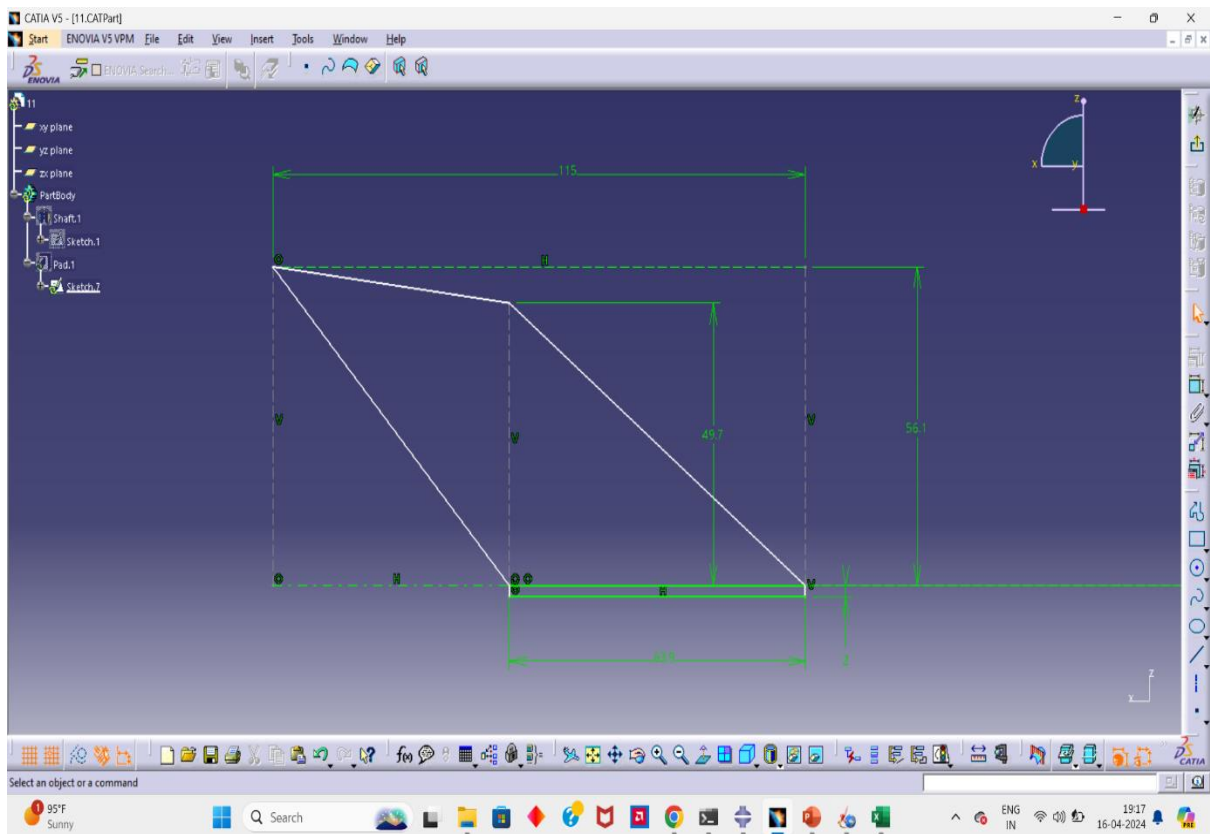


Figure 1. (c) Trapezoidal Fin design.

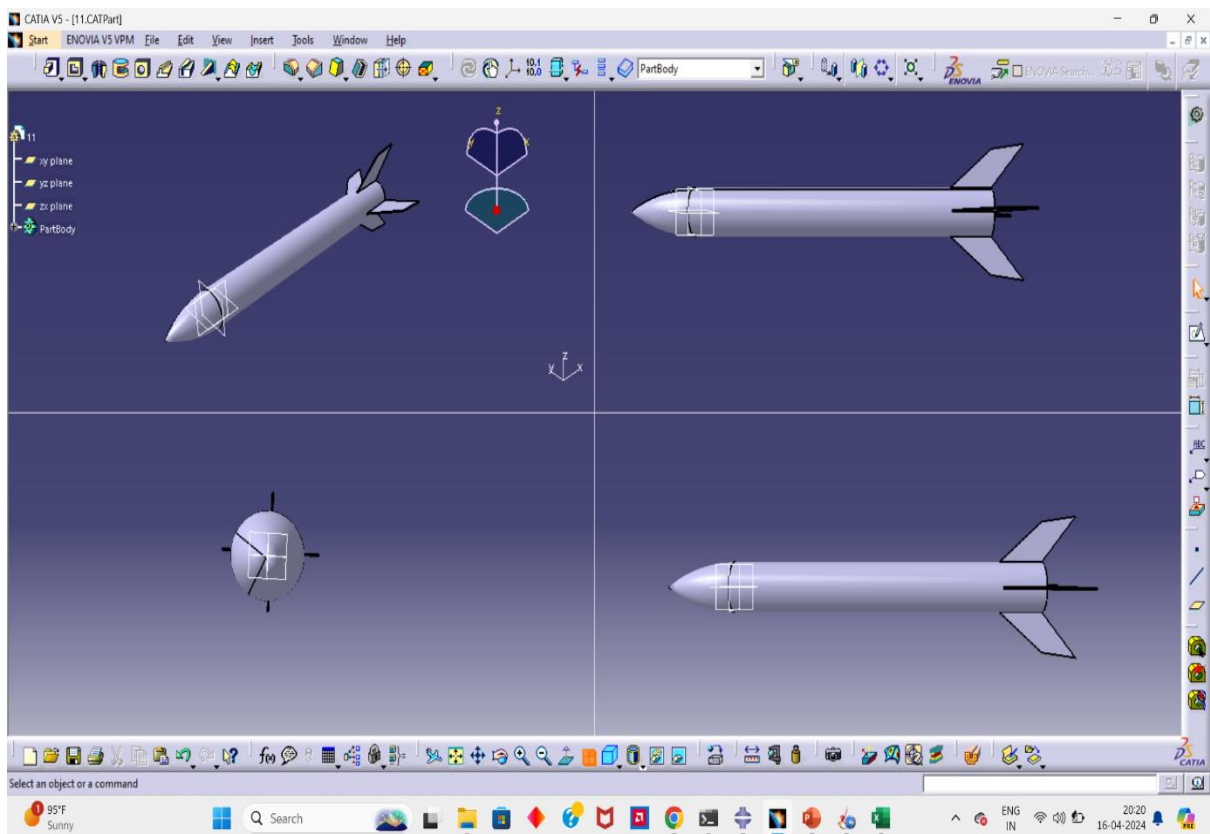


Figure 1. (d) Final design of the rocket.

CFD ANALYSIS

Computational fluid dynamics analysis has revolutionized aerodynamic efficiency evaluation by significantly reducing reliance on costly and time-consuming wind tunnel testing. By simulating airflow and related physics around aerodynamic structures, CFD allows predict and optimize performance outcomes with high accuracy. This modeling provides a detailed understanding of complex interactions, enabling iterative design improvements early in development.

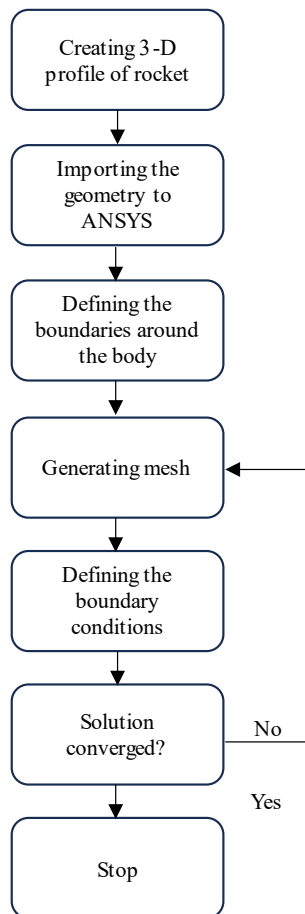


Figure 2. Flowchart of CFD Analysis

As a result, CFD not only speeds up the design process, but also improves the aerodynamic efficiency of products from high-speed aircraft to streamlined automobiles, reducing costs and optimizing performance. ANSYS is a leading software suite widely utilized for CFD analysis [16]. It offers a comprehensive platform for simulating fluid flow, heat transfer, and related phenomena in various engineering applications and the flow chart of CFD analysis has been given in Figure 2.

Meshing

The meshing process for the cuboidal geometry, with dimensions 1.8 m in length, 0.5 m in breadth, and 1 m in height, was conducted using a tetrahedral element type to ensure accurate representation of the geometry and complex stress distribution under analysis. The mesh consists of 40,087 nodes and 128,628 elements, providing a fine discretization to capture detailed responses within the structure. The enclosure around rocket was shown in Figure 3. Tetrahedral elements were selected for their versatility in handling irregular geometries and complex features, ensuring numerical stability and precision. The chosen element density strikes a balance between computational efficiency and result accuracy, making it suitable for advanced simulations. Inflation layer around rocket was shown in Figure 4.

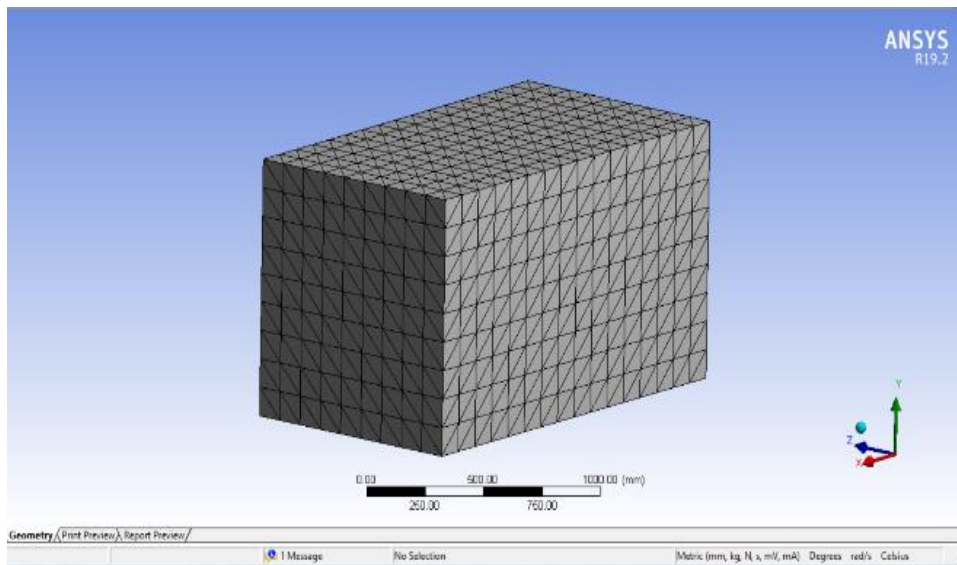


Figure 3. Enclosure around rocket.

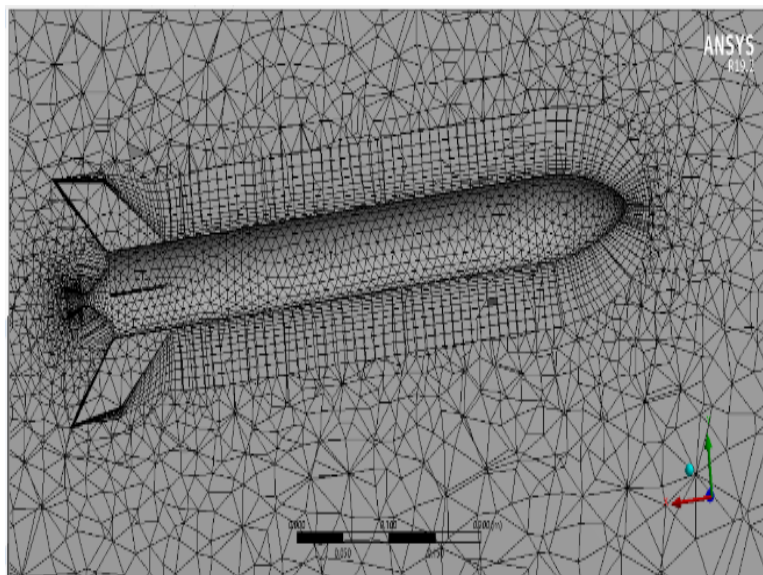


Figure 4. Inflation layer around rocket.

Boundary Conditions

For the computational analysis, a pressure-based solver was employed to solve the governing equations, ensuring robust handling of incompressible flow scenarios. The viscous SST (Shear Stress Transport) k - ω turbulence model was selected due to its effectiveness in capturing near-wall flow phenomena and transition effects, providing a precise resolution of boundary layer characteristics. Boundary conditions were defined as follows: a velocity inlet with an inflow speed of 45.9 m/s, a pressure outlet set to zero gauge pressure, and no-slip conditions applied to the walls to account for the interaction between the fluid and solid surfaces. These settings ensure accurate simulation of fluid dynamics and turbulence effects for the given problem.

CFD Contours

As the velocity 45.9 m/s equivalent to 0.14 Mach, the contour of the velocity be seen and observed that the region of high velocity is depicted with red color. From this it can be stated that the first point of flow separation occurs at nose cone, this is the region where the velocity is low and a stagnation point is observed is Figures 5 and 6.

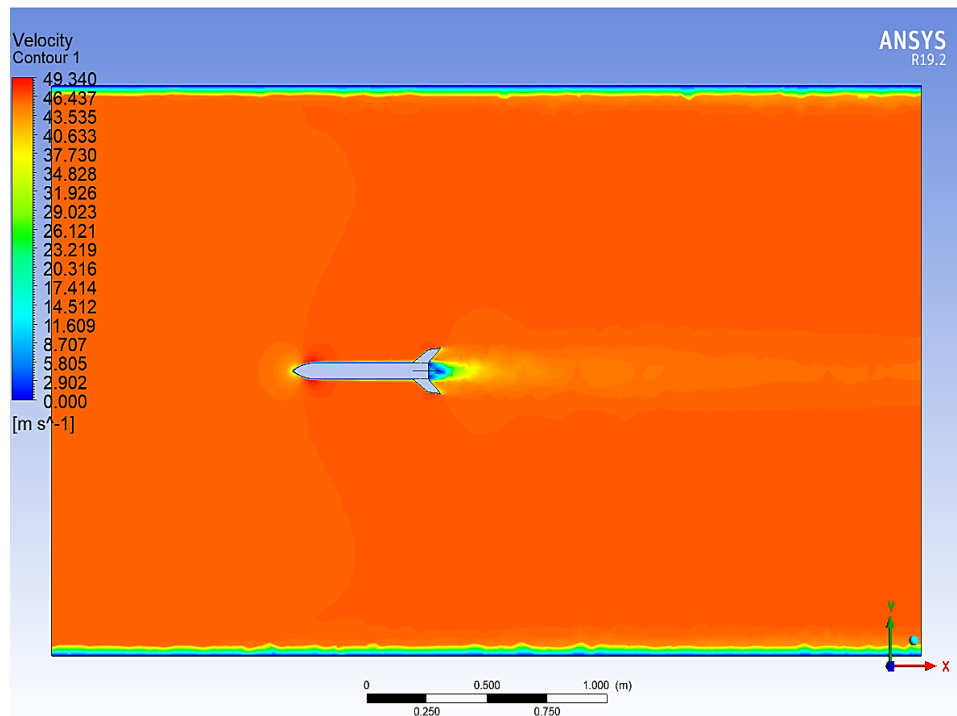


Figure 5. Velocity Contour.

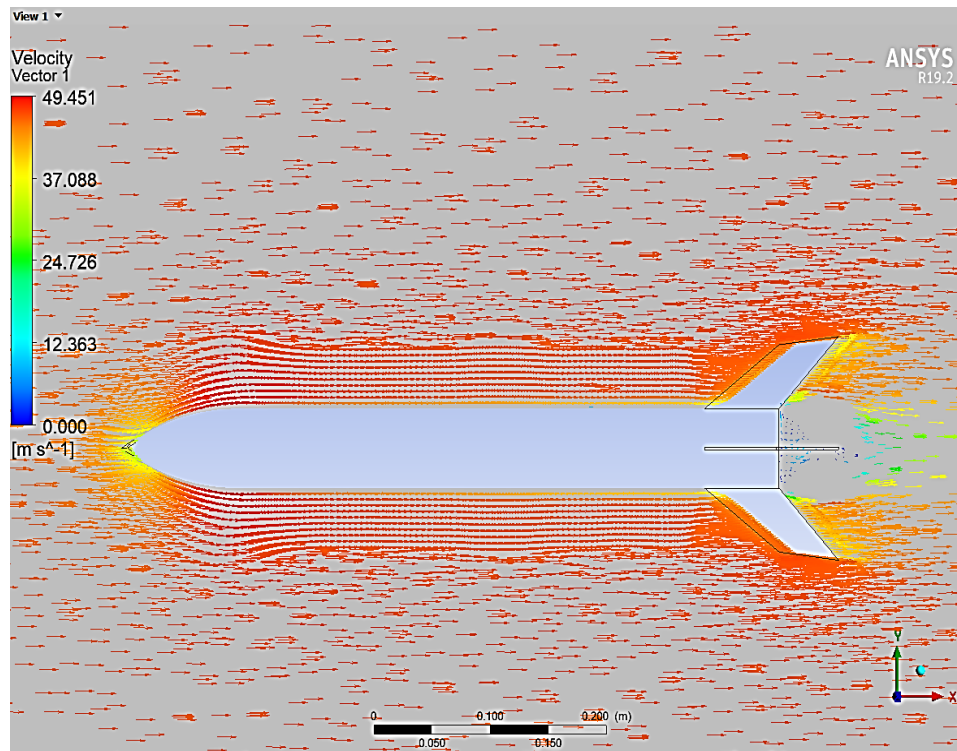


Figure 6. Boundary layer around the rocket.

As explained for the Figure 5, velocity-contour of the nose cone have a stagnation point in the beginning. Consequently, this point depicts that there is maximum pressure occurring at the nose cone. The pressure region at the top and bottom of the rocket are same; which means that there is no lift force. This is because the angle of attack of the rocket for the particular analysis is 0 degrees. A thin boundary layer around the surface of the rocket can be observed in Figure 7.

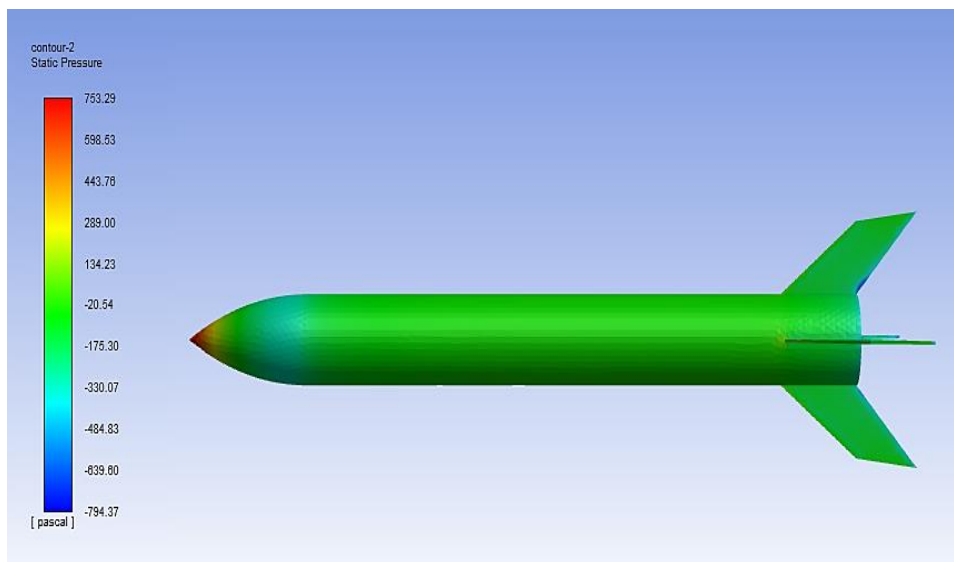


Figure 7. Pressure Contour.

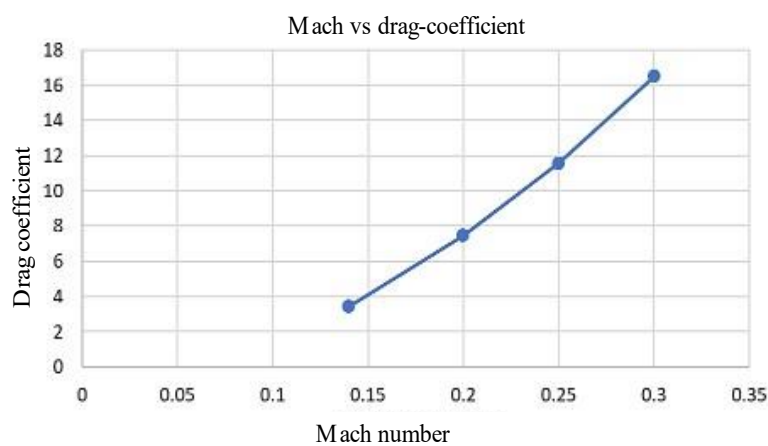


Figure 8. Parametric Study on Mach number.

The results for the different Mach number is investigated for the analysing the drag coefficient acting on the rocket. Four different values of Mach numbers, 0.14, 0.2, 0.25, and 0.3 are used for the turbulence model with low intensity and the viscous model for low $k-\omega$ SST turbulence model is implemented as shown in Figure 8. The results are compared with respect to the drag coefficients obtained. From the parametric study on the Mach number there is an increase in Mach number at approximately 20% which means that the drag coefficient has the increment of nearly 42%. This is an expected result, because as the Mach number increases the velocity also increases and this increase in velocity corresponds to the increment in the drag force on the rocket which could be due to the frictional forces [17]. This affects aerodynamic efficiency by increasing fuel consumption and reducing speed for a given power. At certain angles of attack, increased drag can contribute to greater lift generation, beneficial for maneuvers and takeoff phases in rocket launches.

MATERIAL SELECTIONS

Aerospace constructions are using more and more Fiber Reinforced Polymer Composites (FRPCs), such as Kevlar and Carbon epoxy, because of their better properties over more conventional materials like steel and aluminium. These composites are preferred because of their superior fatigue resistance, remarkable rigidity, and resistance to corrosion. They are also lightweight. Viscoelastic nature of FRPCs is one of their main drawbacks, and it can cause issues in extreme environmental settings. In order to solve this, the incorporation of nano-clay into these composites has been investigated, leading to several

property improvements. Due to photo oxidation effect, exposure to ultraviolet (UV) radiation poses a serious risk to polymeric composites. When UV rays are absorbed, radical chemical groups are formed inside the composite matrix, which starts this process. Material deterioration results from the UV photons' strong enough energy to disrupt molecular bonds in polymers. Often, this deterioration takes the form of fissures, which make it simpler for moisture to enter. Moisture absorption can accelerate the deterioration process of composite materials, impacting their mechanical, chemical, and thermophysical characteristics. A few variables that affect moisture absorption include the surrounding temperature, the strength of the connections that hold the fibres to the matrix, and any defects that result during processing, such as voids or misaligned fibres.

Material Orientation

The alignment of materials in composite structures is fundamental in determining both their strength and stiffness. Simply altering the orientation of the material layup allows for adjustments in strength and stiffness. Woven fibre composites consist of fibres interlaced in a crisscross pattern, providing strength and stiffness in multiple directions. This arrangement allows woven composites to distribute loads more evenly, offering improved resistance to forces acting from various angles. Rockets face complex forces during ascent, including aerodynamic pressures, gravitational forces, and engine thrust, which requires a material capable of effectively withstanding stresses from all directions [18]. Woven fibres excel in this regard and are chosen for the analysis. Their interlaced pattern ensures strength and stiffness in multiple directions, crucial for maintaining structural integrity under varying load conditions.

Carbon Fibre

Carbon Fiber Reinforced Polymer (CFRP) composites have gained popularity in engineering applications for several reasons: Outstanding stiffness-to-weight ratio, Flexibility in advanced material systems Economical and lightweight solutions Simplified production of intricate designs Improved overall material characteristics .However, there are significant challenges associated with these materials: Inherent viscoelastic properties of polymers Sensitivity to extreme environmental conditions Susceptibility to UV radiation, which can alter chemical compositions and degrade material integrity [19].

Table 1. Hashin Damage Criterion of materials

Hashin damage (MPa)	Carbon Fiber	Kevlar Fiber
Longitudinal tensile strength (X^T)	512.3	360
Longitudinal compressive strength (X^C)	330	360
Transverse tensile strength (Y^T)	512.3	360
Transverse compressive strength (Y^C)	330	360
Longitudinal shear strength (S^L)	76.8	105
Transverse shear strength (S^T)	76.8	105

Table 2. Damage Criterion of material.

Damage evolution (N/mm)	Carbon Fiber	Kevlar Fiber
Longitudinal tensile fracture energy	0.01	8.42×10^{-6}
Longitudinal compressive fracture energy	0.01	8.42×10^{-6}
Transverse tensile fracture energy	0.01	8.42×10^{-6}
Transverse compressive fracture energy	0.01	8.42×10^{-6}

Kevlar Fibre

Kevlar epoxy composite is a popular material choice for various applications due to its unique blend of properties: High strength-to-weight ratio, Impact resistance capabilities, and Low thermal

conductivity suitable for applications requiring thermal insulation [20]. Kevlar and epoxy can degrade over time when exposed to UV radiation, extreme temperatures, or harsh chemicals. Moisture Sensitivity: Epoxy resin can absorb moisture, which can affect its mechanical properties. Table 1 and 2 shows the hashin damage criteria and damage evolution of carbon and Kevlar fibre.

Introduction to ABAQUS

Abaqus is a powerful software suite used for finite element analysis (FEA), a computer-based technique for simulating the behaviour of engineering structures. Originally released in 1978, it's known for its robustness and ability to handle complex real-world problems across various industries. Abaqus offers a user-friendly interface for defining models, setting material properties, applying loads, and visualizing results. It offers both pre-processing (model creation) and post-processing (analysis of results) within a unified environment. With a vast library of element types and material models, Abaqus allows engineers to simulate a wide range of physical phenomena, making it a valuable tool for designing and analysing structures.

Meshing the Model

Meshing is crucial in computational simulations because it divides a complex geometry into smaller, manageable elements, enabling precise calculations of variables like stress, heat, and fluid dynamics. Proper meshing ensures accuracy and efficiency in solving engineering and scientific problems, enhancing the reliability and performance of the structure [21]. Figure 9 shows the details of particular structured mesh generated on the model in the Abaqus6.14 software. Element type: S3: a general-purpose, triangular, three-node shell. The number of elements are 62232. Seed size: 2 mm (for whole model).

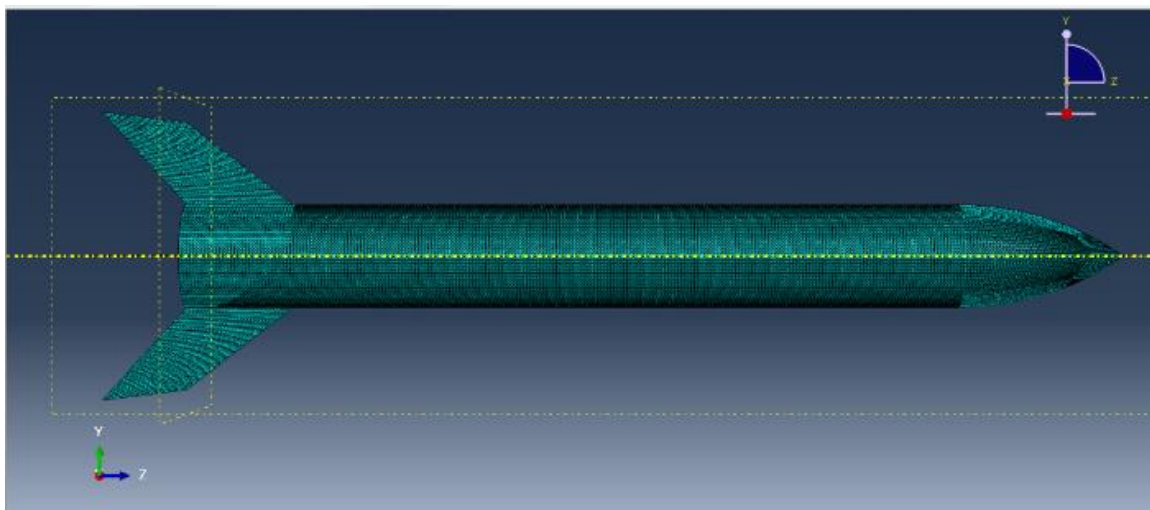


Figure 9. Meshed rocket.

Composite Layup

The layer of composites is modelled in the orientation angle: 0/90/-45/45 for the Carbon and Kevlar fibres was shown in Figure 10 and 11. A combination of Carbon and Kevlar fibre is also modelled in the orientation. Thickness of each ply of the composite is 0.1 mm

	Ply Name	Region	Material	Thickness	CSYS	Rotation Angle	Integration Points
1	✓ Ply-1	(Picked)	cfrp	0.1	<Layup>	0	3
2	✓ Ply-2	(Picked)	kfrp	0.1	<Layup>	90	3
3	✓ Ply-3	(Picked)	cfrp	0.1	<Layup>	-45	3
4	✓ Ply-4	(Picked)	kfrp	0.1	<Layup>	45	3

Figure 10. Composite Layup orientation.

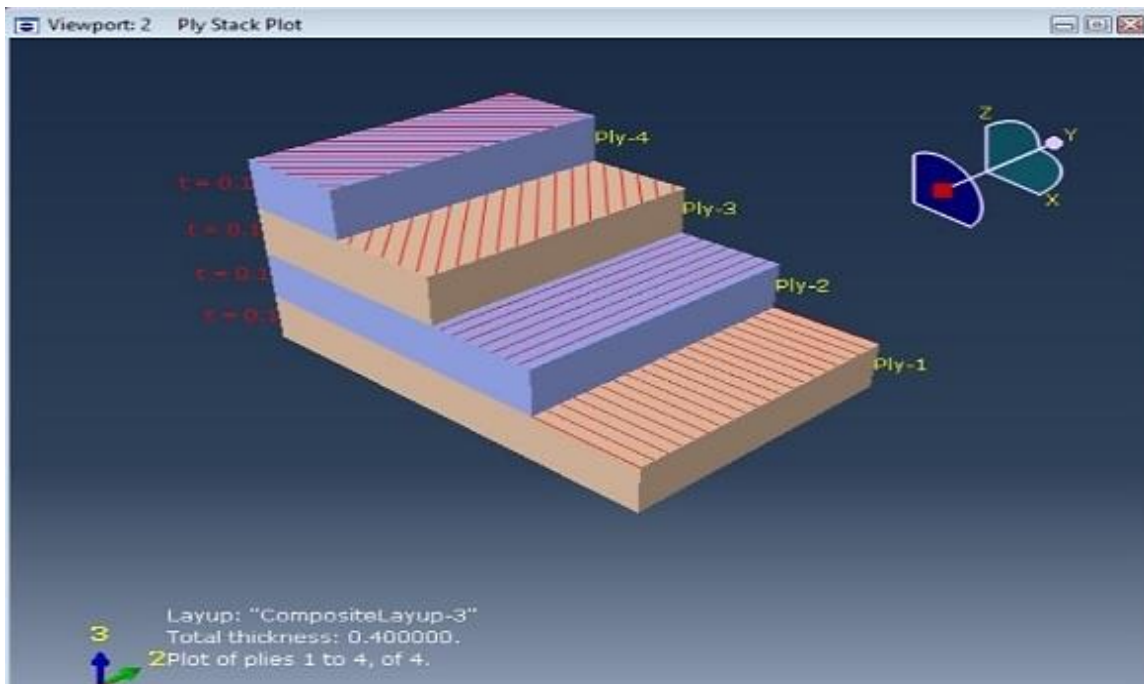


Figure 11. Layup of Carbon-Kevlar Composite

Loading Conditions

The analysis is conducted by applying same aerodynamic loads on the Carbon-fibre composite, Kevlar-fibre composite and Carbon-Kevlar composite as shown in Figure 12. Applying the same loads, boundary conditions, and restrictions to the model for each material and taking them into consideration independently allows for comparison. The problem's boundary conditions are displayed in the graphic of surface loads applied on the rocket. In addition, aerodynamic pressure loads are applied to the rocket. The size of the arrows indicates the magnitude of the load [22]. A distributed pressure load is applied on the surface of rocket; user-defined analytical field is applied taken from the aerodynamic static pressure load from the CFD analysis.

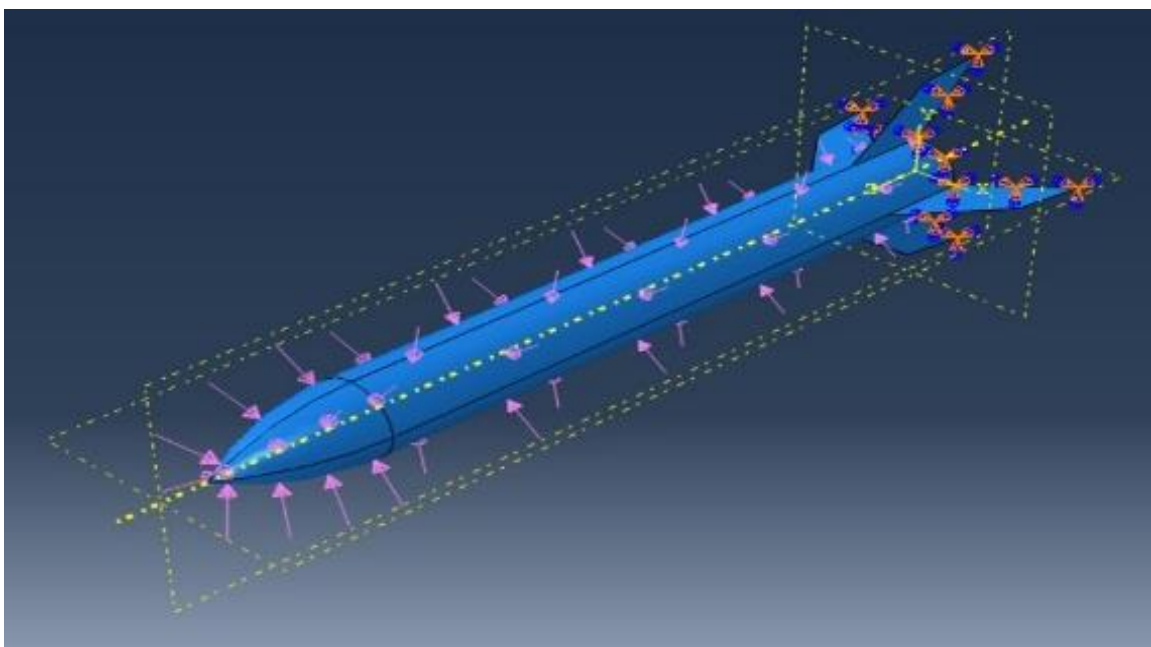


Figure 12. Surface load applied on the structure.

RESULTS AND DISCUSSION

Static analysis conducted for the Carbon-fibre composite, Kevlar-fibre composite and Carbon-Kevlar fibre composite and the results obtained are presented in this section. Static analysis refers to a computational method used to predict the behaviour of structures or components under static loading conditions. It is a fundamental approach employed in engineering simulations to analyse how structures respond to applied forces, moments, or constraints, without considering the effects of time-dependent or dynamic loads.

Static Analysis of Kevlar Fibre Composite

The simulation results from Abaqus illustrate the von Mises stress distribution along the projectile, with a maximum stress (~ 315.911 MPa) observed near the nose section, likely due to high-pressure impact or aerodynamic forces as shown in Figure 13 and 14. The stress decreases progressively toward the tail, as indicated by the color gradient.

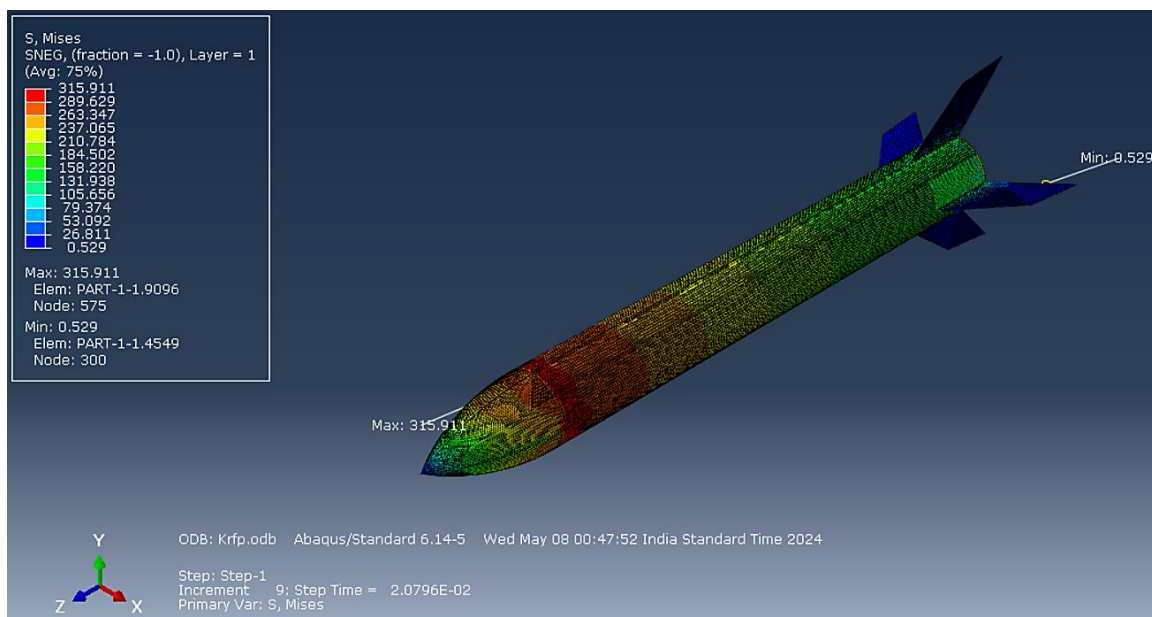


Figure 13. Stress in the structure (Max = 315.91 MPa).

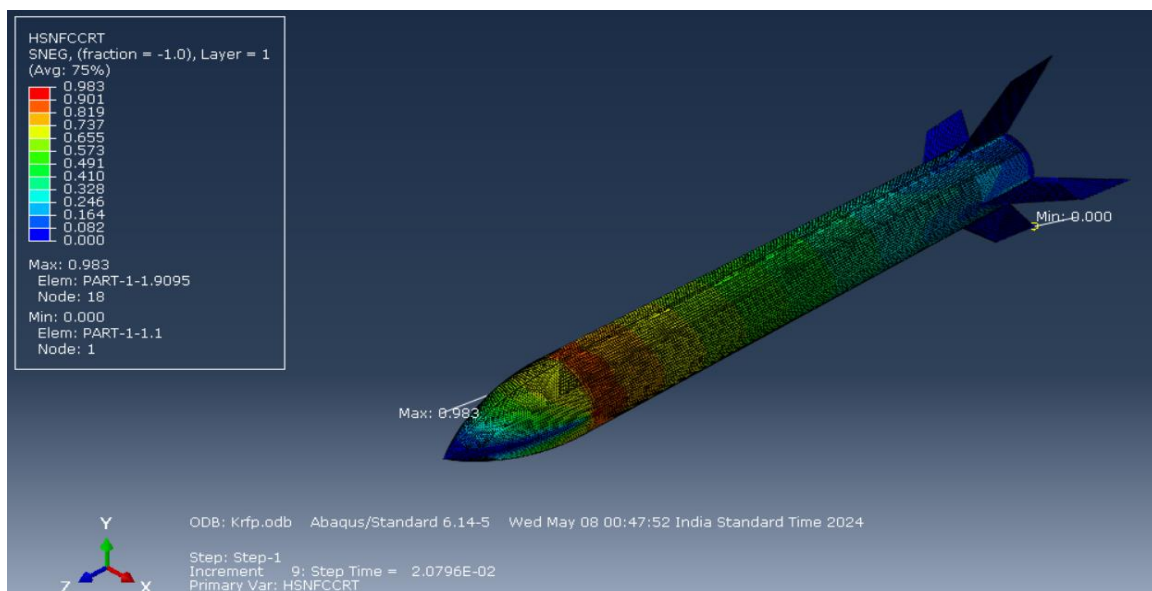


Figure 14. Hashin's Damage initiation (Max = 0.983).

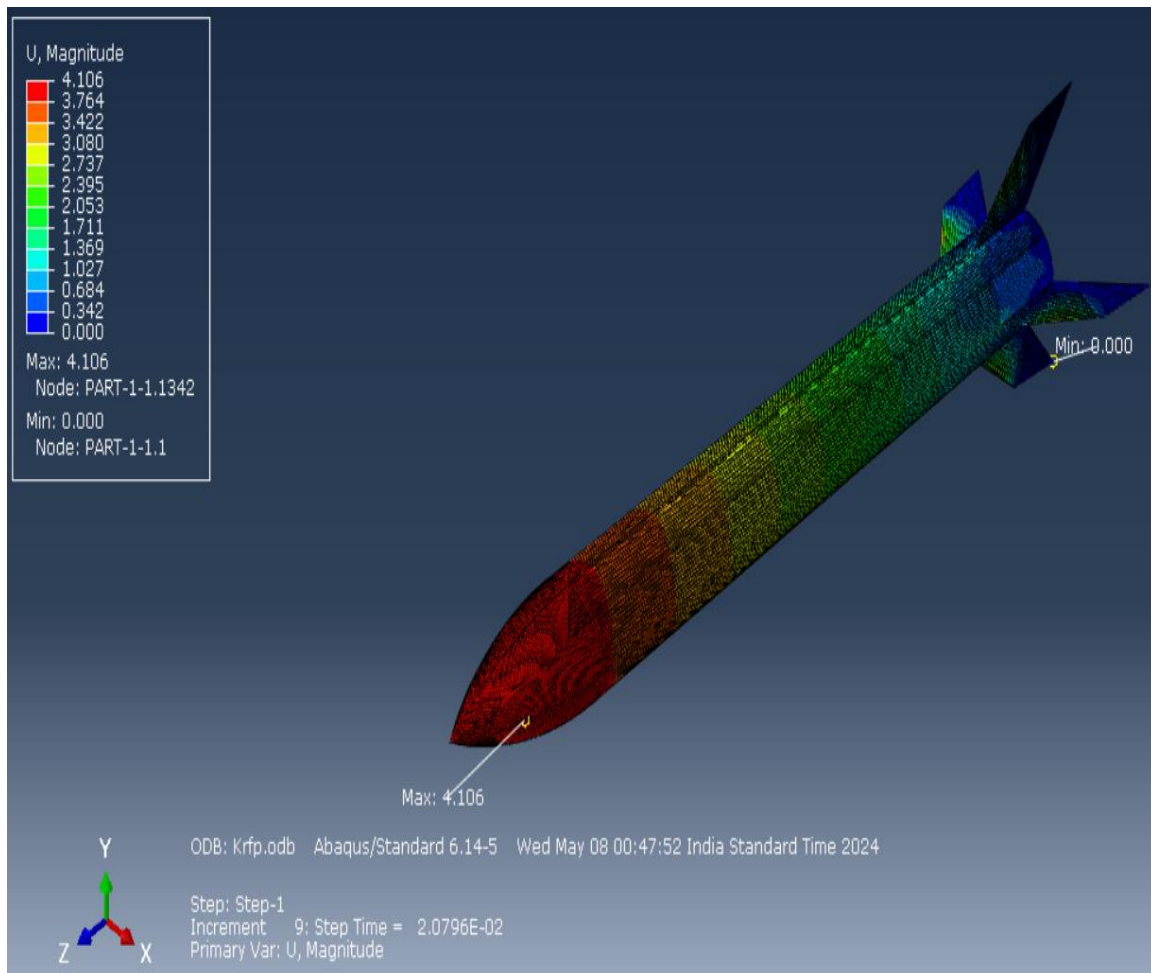


Figure 15. Displacement of the structure (Max = 4.106 mm).

This highlights the nose region as a critical area requiring stronger or reinforced materials to prevent failure. The stress propagation from the front to the rear suggests a well-defined load path, emphasizing the need for structural optimization to maintain integrity during impact or flight. Such analysis is crucial for evaluating the performance and durability of projectiles under dynamic conditions [23]. The simulation Figure 15, illustrates Hashin's damage initiation, with the maximum damage occurring at the nose of the projectile, indicating it as the most critical region under loading. The damage fraction reduces along the body toward the tail, showing lower risk of material failure in those areas. This emphasizes the need for material reinforcement at the nose to improve structural resilience.

Static analysis of Carbon-Kevlar Fibre

The static analysis results for the three materials used in the rocket structure - Kevlar fibre, Carbon fibre, and Carbon-Kevlar fibre Composite reveal significant insights into their structural strength and stability to withstand stresses. Kevlar fibre, while having the highest maximum displacement of 4.106 mm, suggests it may deform more under load, potentially absorbing energy better but also indicating less stiffness compared to the other materials. Carbon fibre showed the lowest maximum Von Mises stress (290.811 MPa) and displacement (1.333 mm), highlighting its superior strength-to-weight ratio and stiffness, which makes it highly effective at resisting mechanical stresses with minimal deformation. The Carbon-Kevlar fibre composite, exhibiting stress levels close to those of Carbon fibre and shows marginally higher displacement in Figures 16 and 17. Structural response characterized by higher stress concentrations at the front and stable regions toward the rear as shown in Figure 18.

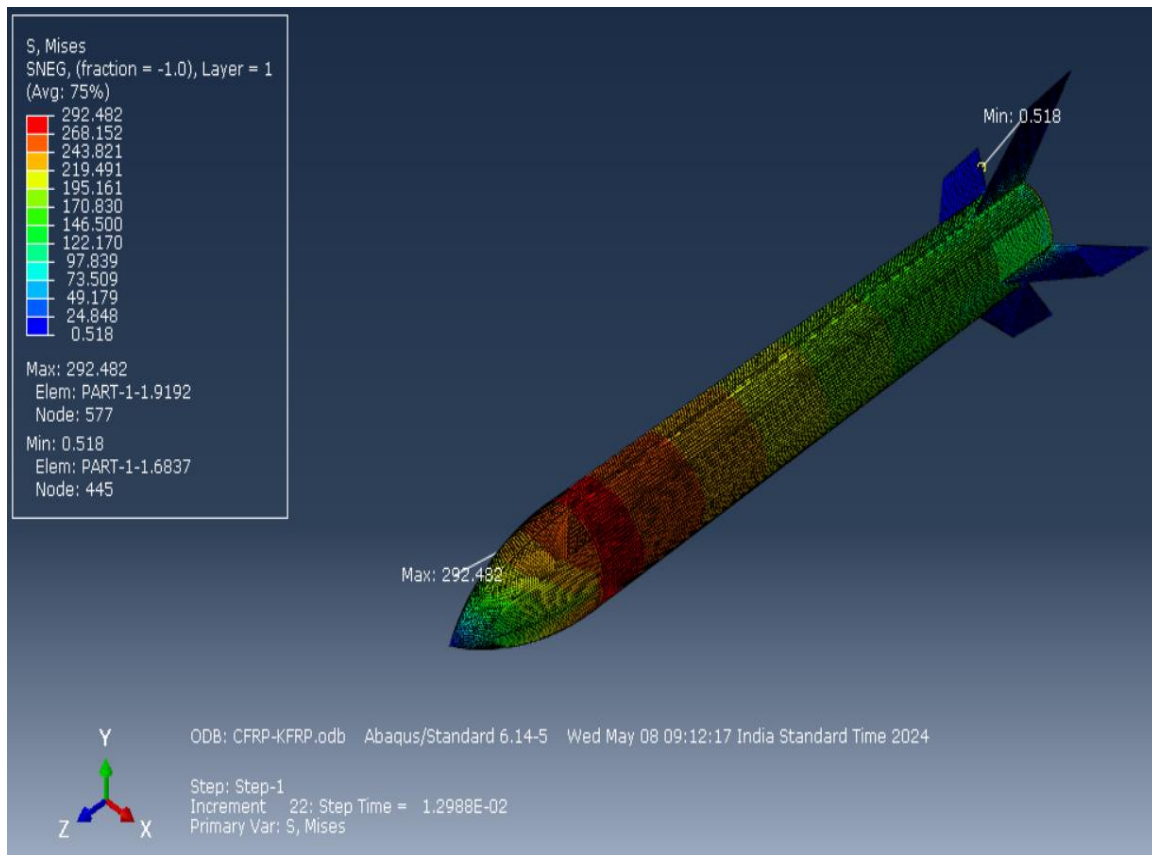


Figure 16. Stress in the structure (Max = 292.48 MPa).

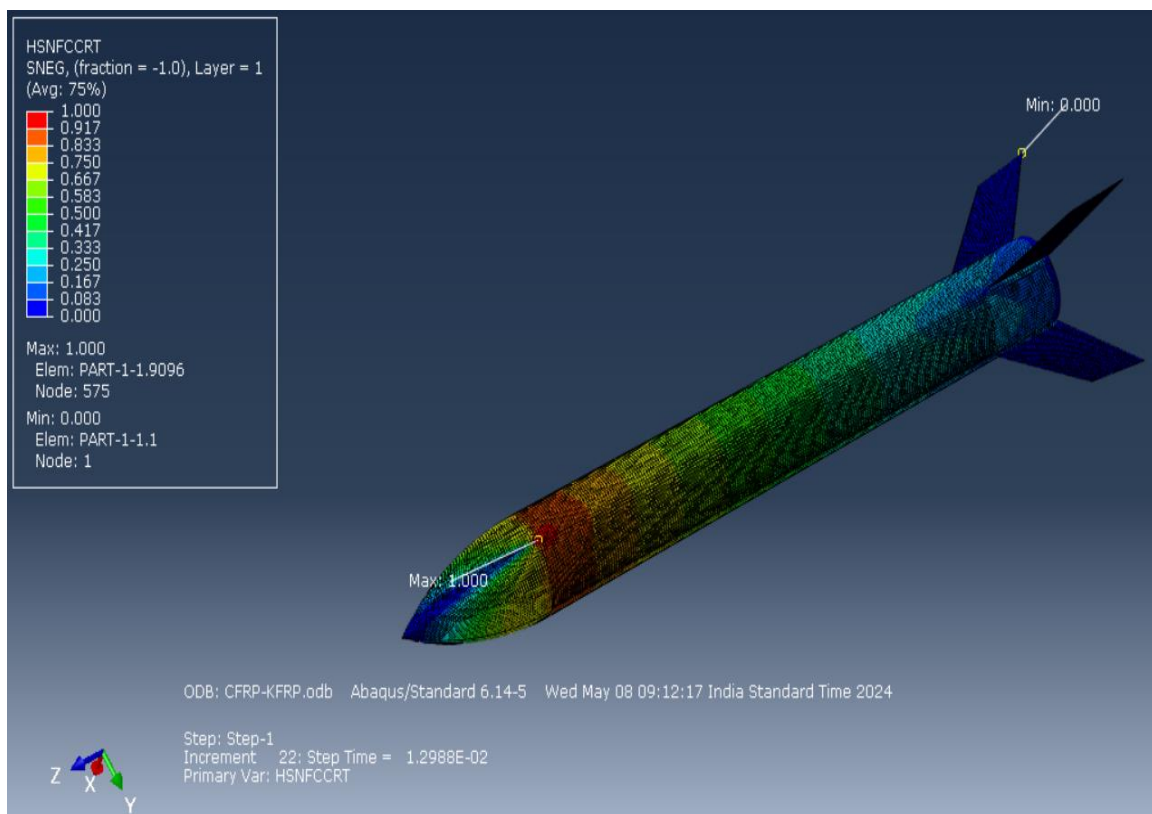


Figure 17. Hashin's Damage initiation (Max = 1).

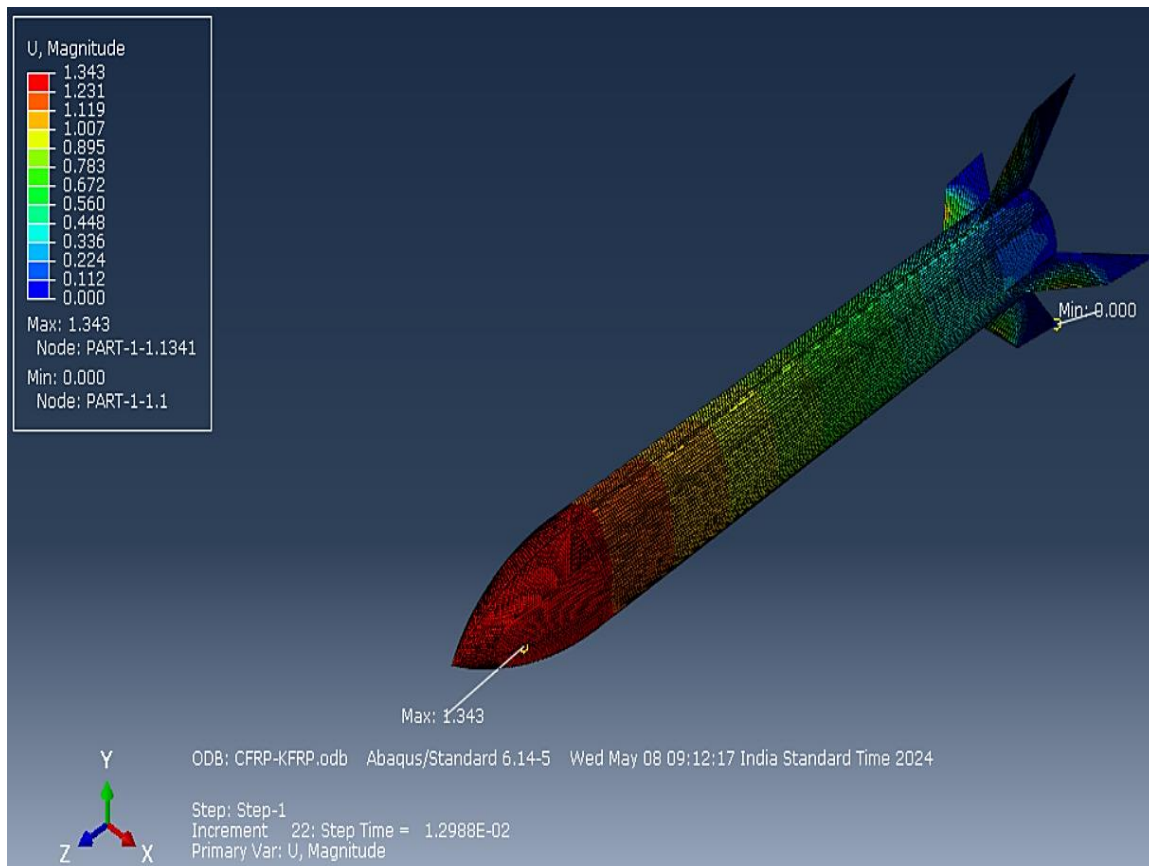


Figure 18. Displacement in the structure (Max = 1.343).

Figure 19 shows the stress-strain curve for Kevlar fibre demonstrates a gradual increase in stress with strain. At a strain of 0.000186087, Kevlar fibre reaches a maximum stress of 278.84 MPa before failure. The material exhibits high elongation and energy absorption capacity, with a strain at failure of approximately 0.000186087. Kevlar fibre offers impact resistance and flexibility, making it ideal for applications requiring high toughness and energy absorption [24]. Whereas, the stress-strain curve for Carbon fibre exhibits high initial stiffness. At a strain of 0.0000823, carbon fibre reaches a maximum stress of 269.934 MPa before failure. This indicates that carbon fibre offers exceptional strength and stiffness, making it suitable for applications where lightweight and high-performance materials are required. Carbon-Kevlar composite reaches a maximum stress of 278.84 MPa before failure at a strain of 0.000186087. This composite exhibits a combination of properties from both carbon fibre and Kevlar fibre, resulting in a balance between stiffness and toughness.

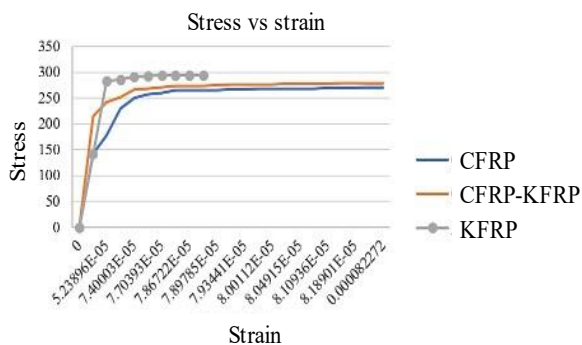


Figure 19. Stress - Strain curve.

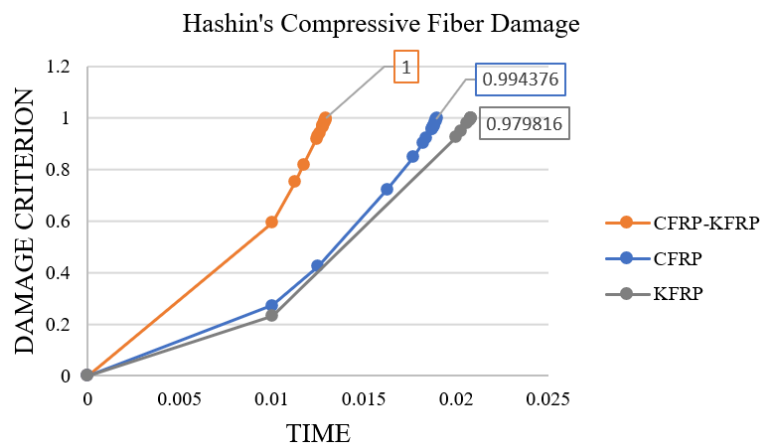


Figure 20. Hashin's compressive damage in fiber.

Hashin's criterion offers a continuous measure of damage accumulation within a material as shown in Figure 20. It considers multiple failure modes, such as fibre breakage, matrix cracking, and delamination, and provides a quantitative measure of damage evolution. In Hashin's criterion, damage is typically represented as a scalar value ranging from 0 to 1, where 0 signifies no damage, and 1 indicates complete failure. As the material undergoes loading, the damage value increases, reflecting the accumulation of microstructural damage and degradation of material properties. The Hashin's compressive fibre initiation criterion for Kevlar fibre shows a rapid increase shortly after the start of the analysis. At a relatively early stage, the criterion reaches a value close to 1, indicating rapid fibre initiation and potential failure under compressive loading. This suggests that Kevlar fibre exhibits high susceptibility to fibre initiation and failure under compressive loading conditions. For the Carbon fibre composite material, the damage criterion increases over time, indicating the progression of fibre failure. However, the rate of increase in the criterion appears to be slower compared to the Carbon-Kevlar composite material. The damage criterion for Carbon-Kevlar composite reaches its maximum value of 1, indicating complete fibre initiation under compressive loading. This suggests that the composite material exhibits progressive damage accumulation, with the initiation of fibre failure occurring over time, ultimately leading to complete failure under compressive loading conditions. Based on the results obtained from the static analysis on the rocket structure in Abaqus, the Carbon fibre material is taken under consideration for further application in the rocket structure. It experienced the lowest maximum stress among the three materials. This indicates that Carbon fibre is subjected to lower levels of mechanical loading compared to Kevlar fibre and the Carbon-Kevlar fibre Composite. Lower stress levels are desirable as they can potentially reduce the risk of material failure and increase structural integrity [25]. Carbon fibre exhibited a lower maximum displacement which indicates that it undergoes less deformation under applied loads

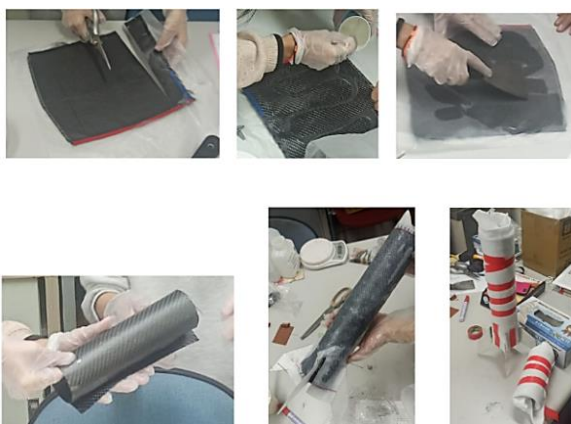


Figure 21. Fabrication of rocket body.



Figure 22. Testing of rocket.

The carbon fiber is used in the fabrication of the rocket. Figure 21 depicts the application and layout of the fiber. Each step, from material selection to fabrication techniques is executed with the goal of maximizing strength and reducing weight. Figure 22, showcases the rigorous testing procedures undergone by the rocket, including parachute deployment and ignition tests. These tests are crucial for verifying the structural integrity and functionality of the rocket under simulated flight conditions.

CONCLUSION

The work was aimed to perform aerodynamic and structural analysis on the rocket case while comparing with two different materials such as Carbon epoxy and Kevlar epoxy to provide with a best suitable material for the rocket structure. The aerodynamic analysis of the rocket conducted in ANSYS Fluent reveals that increasing Mach numbers from 0.14 to 0.3 significantly raises drag coefficients due to higher velocities and resultant frictional forces. However, at certain angles of attack, this increased drag helps generate additional lift, advantageous for rocket phases like manoeuvres and take-off. The results of the static structural analysis conducted in ABAQUS 6.14 shows that carbon-fibre can be able to perform better over that of Kevlar fibre and carbon-Kevlar fibre as noted from the results of analysis, the deformation occurred on carbon fibre is less when applied same loading. The carbon fibre composite material was chosen and fabricated for the rocket structure. Further research recommendation is to conduct experimental analysis using high-level compressive testing machine.

REFERENCES

1. G. Srinivas and M. V. S. Prakash, "Aerodynamics and flow characterisation of multistage rockets," in *IOP Conf. Ser.: Mater. Sci. Eng.*, vol. 197, p. 012077, IOP Publishing, 2017.
2. Z. Aytac, F. Aktas, "Utilization of CFD for the Aerodynamic Analysis of a Subsonic Rocket," *Journal of Polytechnic*, vol. 23, no. 3, pp. 879–887, 2020.
3. A. Fedaravičius, S. Kilikevičius, and A. Survila, "Investigation on the aerodynamic characteristics of a rocket-target for the system 'Stinger'," *Journal of Vibroengineering*, vol. 17, no. 8, pp. 1854, Dec. 2015.
4. N. Sahbon et al., "CFD study of base drag of the GROT rocket," *Transactions on Aerospace Research*, vol. 271, no. 2, pp. 1–16, 2023.
5. N. L. Tun et al., "Aerodynamic coefficients prediction for 122 mm rocket by using computational fluid dynamics," in *IOP Conf. Ser.: Mater. Sci. Eng.*, vol. 816, p. 012010, IOP Publishing, 2020.
6. J. Peng et al., "Numerical simulations on aerodynamic characteristics of a guided rocket projectile," in *3rd International Conference on Materials Engineering, Manufacturing Technology and Control (ICMEMTC 2016)*.
7. H. P. Manimaran et al., "Stability analysis of conventional rocket model using CFD tool," *International Journal of Engineering Research & Technology (IJERT)*, vol. 9, no. 01, pp. 262, Jan. 2020.
8. M. N. Dahalan et al., "Aerodynamic study of air flow over a curved fin rocket," *Journal of Advanced Research in Fluid Mechanics and Thermal Sciences*, vol. 40, no. 1, pp. 46–58, 2017.

9. J. C. Robinson and D. O. Stanley, "Structural and load analysis of a two-stage fully reusable advanced manned launch system," in *Fourth AIAA/USAF/NASA/OAI Symposium on Multidisciplinary Analysis and Optimizations*, Sep. 21–23, 1992.
10. A. Thankachen and S. Kumar, "Design optimization and analysis of rocket structure for aerospace applications," *International Journal of Engineering Trends and Technology (IJETT)*, vol. 24, no. 6, pp. 286, Jun. 2015.
11. B. R. Capra, L. M. Brown, and R. R. Boyce, "Aerothermal–Structural Analysis of a Rocket-Launched Mach 8 Scramjet Experiment: Descent," *Journal of Spacecraft and Rockets*, doi: 10.2514/1.A33964.
12. S. Shaheen and G. S. Gupta, "Design and analysis of carbon-epoxy composite rocket motor casing," *International Journal of Advance Research and Innovative Ideas in Education*, vol. 1, no. 5, 2015.
13. J. J. Joshua et al., "Fabrication and experimental estimation of mechanical properties of Kevlar-Glass/Epoxy interwoven composite laminate," *Journal of Nanomaterials*, vol. 2023, pp. 1055071, 2023.
14. K. Kiran and E. R. Cholleti, "Static aeroelastic analysis on two-stage rocket body," *International Journal of Engineering Research & Technology (IJERT)*, vol. 4, no. 11, pp. 423, Nov. 2015.
15. M. A. Habaka et al., "Experimental and computational dynamic structural analysis of free-flight rockets," in *IOP Conf. Series: Materials Science and Engineering*, vol. 973, p. 012021, IOP Publishing, 2020.
16. Adnan, A., Hamid, A.H.A., Salleh, Z. and Azizi, M.Z., 2023. Mathematical and Computational Fluid Dynamics Analysis of Low-Altitude Rocket Drag for Various Fin Configurations. *Journal of Aerospace Engineering*, 19(2), pp.134–142.
17. Chew, I., Taylor, M., Thompson, M., Trine, K., Worosz, M. and Canino, J., 2023. Methods for modeling and Controlling the Flight Path of a High Power Rocket. In *2023 Regional Student Conferences* (p. 72413).
18. Steppert, M. and Epple, P., 2017, November. Numerical investigation of the drag of rockets at subsonic, transonic and supersonic speeds. In *ASME International Mechanical Engineering Congress and Exposition* (Vol. 58424, p. V007T09A074). American Society of Mechanical Engineers.
19. Kesuma, P., Darmawan, S. and Halim, A., 2020, December. Aerodynamics analysis of mobil irit tarumanagara using CFD method. In *IOP Conference Series: Materials Science and Engineering* (Vol. 1007, No. 1, p. 012032). IOP Publishing.
20. Srinivas, G. and Prakash, M.V.S., 2017, May. Aerodynamics and flow characterisation of multistage rockets. In *IOP Conference Series: Materials Science and Engineering* (Vol. 197, No. 1, p. 012077). IOP Publishing.
21. Garud, P. and Ajluni, R., 2024. Torsional Stiffness Testing and Analysis of Composite Double wedge Rocket Fins. In *2024 Regional Student Conferences* (p. 84867).
22. Chavda, K.J., 2024. Using the Drag Equation and Euler's Method in Python to Predict Model Rocket Flight Trajectories. In *2024 Regional Student Conferences* (p. 84150).
23. Karlekar, C. and Barve, S.B., 2024. Design of rotation inducing rocket fins and their analysis for aerodynamic stability. *Aerospace Systems*, pp.1–6.
24. Sankalp, S.S., Sharma, V., Singh, A., Salian, A.S. and Srinivas, G., 2022. Computational analyses of tail fin configurations for a sounding rocket. *Aerospace Systems*, 5(2), pp.233–246.
25. Masot Carrero, V., 2024. *Numerical characterization of the aerodynamics and trajectory of a rocket* (Doctoral dissertation, Universitat Politècnica de València).